Existence of k^{-1} power-law scaling in the equilibrium regions of wall-bounded turbulence explained by Heisenberg's eddy viscosity

Gabriel G. Katul,[1,2] Amilcare Porporato,[1,2] and Vladimir Nikora[3]

[1]*Nicholas School of the Environment, P.O. Box 80328, Duke University, Durham, North Carolina 27708*

[2]*Department of Civil and Environmental Engineering, Duke University, Durham, North Carolina 27708*

[3]*The School of Engineering, Fraser Noble Building Kings College, Aberdeen AB24 3UE, Scotland, United Kingdom*

(Received 17 December 2011; revised manuscript received 16 October 2012; published 13 December 2012)

The existence of a "−1" power-law scaling at low wavenumbers in the longitudinal velocity spectrum of wall-bounded turbulence was explained by multiple mechanisms; however, experimental support has not been uniform across laboratory studies. This letter shows that Heisenberg's eddy viscosity approach can provide a theoretical framework that bridges these multiple mechanisms and explains the elusiveness of the "−1" power law in some experiments. Novel theoretical outcomes are conjectured about the role of intermittency and very-large scale motions in modifying the k^{-1} scaling.

DOI: 10.1103/PhysRevE.86.066311 PACS number(s): 47.27.−i

I. INTRODUCTION

The spectral properties of turbulence at high wavenumbers have been extensively studied in turbulent flows, and existing theories appear satisfactory in describing their basic statistical properties at very high Reynolds numbers [1–4]. Equivalent theories for the low wavenumber range have been comparatively lacking because boundary conditions prohibit the attainment of universal behavior. Among the few theories proposed at low wavenumbers is a k^{-1} scaling in the longitudinal (u) velocity spectrum $E_u(k)$ at wavenumbers ($kz \leqslant 1$) of wall-bounded flows, where z is the height from the boundary and k is the wavenumber. This scaling behavior was observed in numerous boundary-layer studies (reviewed in Ref. [5]) and in Large Eddy Simulations of the neutral atmospheric boundary layer [6–8]. Tchen [9,10] was the first to theoretically predict the k^{-1} scaling via a spectral budget equation. Other approaches resulting in a k^{-1} power law include dimensional analysis or asymptotic matching between the so-called inner and outer regions of the velocity spectra [11–14]. Nikora [15] later showed that one possible mechanism for generating a k^{-1} scaling at a given z can be explained by superposition of Kolmogorov cascades generated at all possible distances from the ground above z. This superposition argument leads to a turbulent kinetic energy flux equal to the dissipation rate at wave numbers larger than $1/z$ that scales as $\bar{\varepsilon} \sim u_*^3 k^1$ for $kz \leqslant 1$. When this scaling is combined with the well-celebrated Kolmogorov energy cascade ($E_u \sim \bar{\varepsilon}^{2/3} k^{-5/3}$), it leads to an $E_u \sim u_*^2 k^{-1}$ for $kz \leqslant 1$, where overbar is time-averaging, $\bar{\varepsilon}$ is the mean turbulent kinetic energy dissipation rate, $u_* = (\tau_t/\rho)^{1/2}$ is the friction velocity, τ_t is the turbulent stress, and ρ is the mean fluid density. The assumption that τ_t is independent of z is reasonable for a zero-mean pressure gradient flow that is stationary, planar-homogeneous, at very high Reynolds number, and in the absence of any subsidence.

Interest in the onset of the k^{-1} power-law scaling in $E_u(k)$ has resurfaced following new experiments and analyses, including the super-pipe high Reynolds number flow experiments that showed no clear k^{-1} power-law scaling [16]. Another laboratory boundary layer experiment [17] suggested that a prerequisite to the emergence of a k^{-1} power-law scaling in $E_u(k)$ marked by at least one decade of scales is not only limited to a very large Reynolds number ($H^+ = H u_*/\nu > 50\,000$), as was the case for the super-pipe experiment. Additional constraints were proposed, including a dimensionless height from the boundary $z^+ = z u_*/\nu > 100$ so as to avoid any viscous effects and $z/H \leqslant 0.02$ to ensure a minimum overlap zone between the inner and outer regions in which the k^{-1} scaling is presumed to emerge [17], where H is the boundary-layer height, and ν is the kinematic viscosity. Other recent studies [14,18,19] questioned the use of a spectral budget approach as lacking any accounting for a rigid boundary. The scaling analysis in Ref. [15] was also criticized for ignoring coherent structures, although implicitly they were considered through the use of Townsend's attached eddies concept. However, the potentially important effects of very large scale motions (VLSM) or superstructures, have not been explored. Another critique of the spectral budget approach and the scaling analysis in Ref. [15] is their prediction of a k^{-1} power law for the vertical velocity spectra $E_w(k)$, which was not reported in previous studies. However, a near k^{-1} scaling in $E_u(k)$ was reported in many experiments despite the fact that the restrictions listed in Ref. [17] were not always satisfied [5].

What is evident is that beyond dimensional analysis and asymptotic arguments, a complete phenomenological theory that bridges these multiple arguments and explains the occurrence or absence of a k^{-1} scaling is lacking. A novel phenomenological spectral theory based on Heisenberg's eddy-viscosity approach [20] is proposed here. It recovers (i) Nikora's [15] scaling arguments for infinite Reynolds number and a deep boundary layer, (ii) aspects of the attached eddy pertinent to the generation of a k^{-1} power law, and (iii) some empirical conditions proposed for the onset of a k^{-1} power law. Using this phenomenological theory, conjectures about the expected role of coherent structures and VLMS as well as intermittency in modifying the k^{-1} power law are also presented.

II. THEORY

The development commences with the turbulent kinetic energy viscous dissipation rate ($\bar{\varepsilon}$) being related to the amplitude of the squared turbulent vorticity ($\overline{\omega_i \omega_i}$) for high

Reynolds number using

$$\overline{\varepsilon} = \nu\overline{\omega_i\omega_i} = 2\nu\int_0^\infty E_{\mathrm{TKE}}(k')k'^2dk', \quad (1)$$

where $E_{\mathrm{TKE}}(k)$ is the total energy spectrum obtained as a sum of the three-dimensional spectra of individual velocity components (u, v, and w) integrated over the surface of a sphere of radius k, where k is the scalar wavenumber, u, v, w are the longitudinal, lateral, and vertical velocity components along directions x, y, and z, respectively, $\int_0^\infty E_{\mathrm{TKE}}(k)dk = \overline{e^2} = (\sigma_u^2+\sigma_v^2+\sigma_w^2)/2$ is the mean turbulent kinetic energy (TKE) related to the sum of the three component velocity variances (σ_u, σ_v, and σ_w), and k' is a dummy integration variable. Heisenberg's argument rests on the assumption that Eq. (1) can be rewritten via a turbulent viscosity to yield (see Appendix)

$$\varepsilon(k) = [\nu+\nu_t(k)]\int_0^k 2\,E_{\mathrm{TKE}}(k')k'^2dk', \quad (2)$$

where $\varepsilon(k)$ is the turbulent kinetic energy dissipation rate at wavenumber k, $\nu_t(k)$ is a wavenumber-dependent turbulent viscosity given as

$$\nu_t(k) = C_H\int_k^\infty\sqrt{\frac{E_{\mathrm{TKE}}(k')}{k'^3}}dk', \quad (3)$$

and C_H is the Heisenberg constant of order unity. The assumption behind Eqs. (2) and (3) is that for all eddies whose wavenumbers are between 0 and k (i.e., large scales), the action of smaller eddies can be represented by an additional turbulent viscosity ν_t that must depend on the energy and wavenumbers of all smaller scale eddies. This ν_t expression does not preclude nonlocal spectral interactions between large and small eddies. When $\nu \ll \nu_t(k_1)$ at a given k_1, Eq. (2) reduces to

$$\int_0^{k_1} 2\,E_{\mathrm{TKE}}(k')k'^2dk' \approx \frac{\varepsilon(k_1)}{C_H\int_{k_1}^\infty\sqrt{\frac{E_{\mathrm{TKE}}(k')}{k'^3}}dk'}. \quad (4)$$

At the wavenumber $k_1 = 1/z$, it can be shown that (see Appendix)

$$\varepsilon(z) = \varepsilon(k_1) = \frac{u_*^3}{k_v z} = \frac{1}{k_v}u_*^3k_1, \quad (5)$$

where $k_v = 0.4$ is the Von Karman constant. The presence of a mean velocity gradient impacting the low-wavenumber range primarily modifies the above result to within a constant as shown in the Appendix. In the Appendix, a simplified spectral budget equation that retains the production term is first considered. A gradient-diffusion approximation in the spectral domain is then used to close the production, which alters the resulting spectrum to within a constant. With this estimate for $\varepsilon(z)$, the spectral budget at this $k_1 = 1/z$ can be expressed as

$$\int_0^{k_1} 2\,E_{\mathrm{TKE}}(k')k'^2dk' = \frac{u_*^3k_1}{k_vC_H\int_{k_1}^\infty\sqrt{\frac{C_o\varepsilon(k_1)^{2/3}k'^{-5/3}}{k'^3}}dk'}. \quad (6)$$

In determining ν_t at very large Reynolds number, the energy spectrum for $k\in[k_1,\infty]$ can be approximated by the Kolmogorov spectrum $C_o\bar{\varepsilon}(z)^{2/3}k'^{-5/3}$ (hereafter referred to as K41), where $C_o \approx 1.55$ is the Kolmogorov constant. It follows that the E_{TKE} for $k\in[0,k_1]$ is given as

$$\int_0^{k_1} 2\,E_{\mathrm{TKE}}(k')k'^2dk' = C_{\mathrm{TKE}}u_*^2k_1^2, \quad (7)$$

where $C_{\mathrm{TKE}} = (4/3)(k_v^{2/3}C_HC_o^{1/2})^{-1}$. Assuming further that E_{TKE} for $k\in[0,k_1]$ is self-similar abiding by an extensive power law given as $E_{\mathrm{TKE}} = Ak^{-a}$, then A and a can be determined by integrating the left-hand side of Eq. (7) and equating the outcome to its right-hand side to yield

$$2A\frac{k_1^{3-a}}{3-a} = C_{\mathrm{TKE}}u_*^2k_1^2, \quad (8)$$

resulting in $a=1$ and $A = C_{\mathrm{TKE}}u_*^2$, and hence $E_{\mathrm{TKE}} = C_{\mathrm{TKE}}u_*^2k^{-1}$ for $kz<1$. The E_{TKE}, not the spectrum of individual velocity components, scales as k^{-1} for $kz\leqslant 1$. This finding does not require that each individual velocity component spectra possess a k^{-1} scaling; only the ones contributing most to the overall TKE [i.e., $E_u(k)$ and $E_v(k)$]. To illustrate why E_u and E_v contribute most to the overall TKE, recall that in the logarithmic region of boundary layers, $\overline{e^2} = \frac{1}{2}(A_u^2+A_v^2+A_w^2)u_*^2$, where $A_u\approx 2.3$, $A_v\approx 2.1$, and $A_w\approx 1.25$. Hence, σ_w^2 contributes under 15% of the total TKE. The $E_w(k)$ generally does not exhibit any k^{-1} scaling due to wall-effects [21]. The considerations presented above are valid for the logarithmic layer where the global TKE production is approximately balanced by its dissipation, and where the inhomogeneity does not contribute significantly to the spectral energy balance (i.e., the energy flux due to the inhomogeneity is constant within the log layer and can be viewed in terms of energy fluxes as a locally homogeneous shear layer [22]).

III. EXPERIMENT

Figure 1 shows measured E_{TKE} (in regular and premultiplied form) computed using orthonormal wavelet transforms (OWT) for flows over a number of surfaces, including a smooth-walled laboratory flume at two heights ($z^+ =$ 55.0, 92.0), an Antarctic ice sheet ($z^+ = 3.6\times10^5$), a grass-covered forest clearing ($z^+ = 1.6\times10^5$), a pine stand ($z^+ = 1.6\times10^5$), and a hardwood forest ($z^+ = 6.6-7.4\times10^5$). These data sets, briefly described next, are also used to explore the scaling laws of E_u and E_w using conventional Fourier transforms to supplement the OWT analysis. For the canopy experiments, the canopy height is denoted by h_c and z is defined from a zero-plane displacement ($2/3\,h_c$). The amount of canopy foliage is characterized by the leaf area index (i.e., foliage area per ground area), denoted by LAI.

A. Flume experiments

The open channel (OC) experiments were conducted at Cornell University in a 20-m-long, 1.0-m-wide, and 0.8-m-deep open channel tilting flume with a smooth stainless steel bed. The channel slope was set at 0.0001 mm^{-1} resulting in an $H = 10.3$ cm of water depth. The longitudinal and vertical velocity components were measured using a two-dimensional split film boundary layer probe (TSI 1287W model). The sampling frequency and period were 100 Hz and 81.92 seconds per flow variable per depth. The velocity measurements were

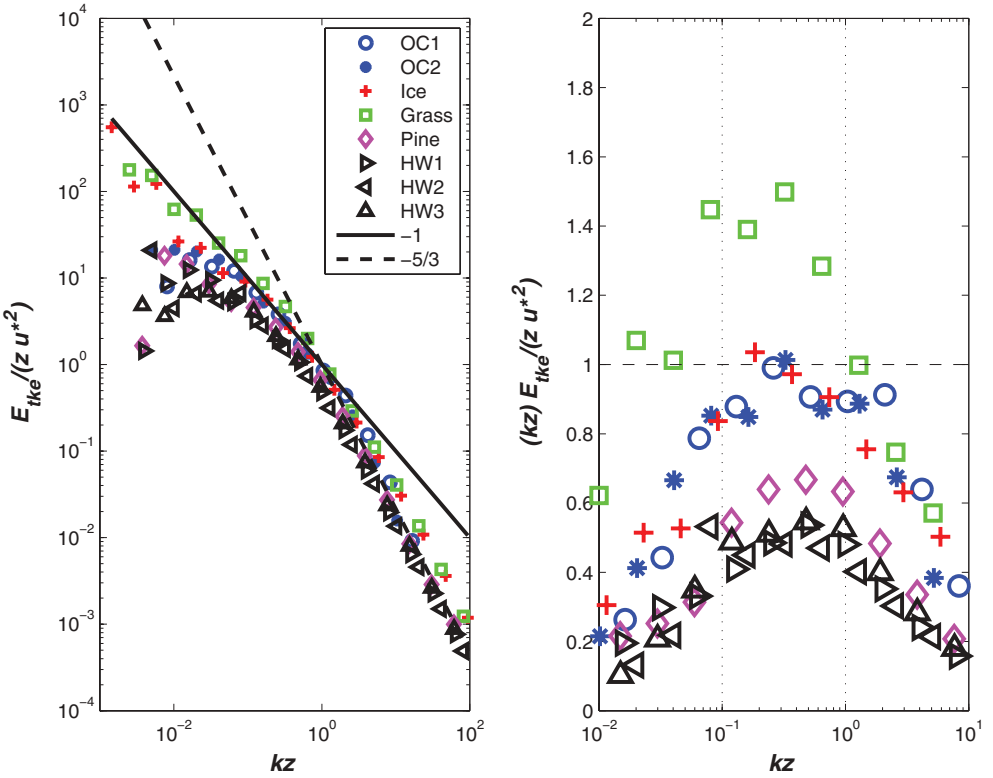

FIG. 1. (Color online) Measured normalized $E_{\mathrm{TKE}}(k)$ (right) using OWT for open channels (open circles, $z^+ = 55$; closed symbol, $z^+ = 92$), ice sheet (plus), grass site (squares), a pine stand (diamond), and a hardwood canopy (triangles for different days). The normalizing velocity and length scales are the measured u_* and z. The -1 (solid) and $-5/3$ (dashed) power laws are shown. The premultiplied spectra for TKE are presented to emphasize the region over which the -1 power law exist (left). Because time is converted to wavenumber space using Taylor's frozen turbulence hypothesis, the wavenumbers shown must be interpreted along the x direction and not three-dimensional. Due to their differencing properties, OWT are less sensitive to nonstationarities when compared to their Fourier counterparts and are preferred for such data sets.

performed at $z = 0.1$, 0.2, 0.3, 0.4, 0.6, and 1 cm from the channel bottom. The turbulent stresses were found to be independent of height from $z = 0.6$ cm to $z = 1$ cm. The friction velocity was determined to be around $u_* = 0.9$ cm s^{-1} using three separate methods that agree to within 10% as discussed elsewhere [5]. The data reported here are for $z = 0.6$ and $z = 1.0$ cm, corresponding to $z^+ = 55$ and $z^+ = 92$. The mean velocity is about 0.2 m s^{-1} and $\sigma_u/u_* = 2.5$ at both heights.

B. Ice sheet

The experiment was conducted from November 12 in 1994 until January 6 in 1995 above the Nansen Ice Sheet (50 by 30 km^2) in a coastal area close to the Terra Nova Bay Italian station in Antarctica. The site experiences frequent katabatic winds flowing from the Antarctic Plateau toward the Ross Sea along the Reeves Glacier. Velocity measurements were performed at 20.8 Hz using symmetric three-axis ultrasonic anemometry (Gill Inst. Ltd.) positioned at $z = 22$ m above the surface (highest measurement level) and described elsewhere [23]. The data reported here are about a 7-h composite run made up of 14 consecutive 30-minute stationary runs with a $u_* = 0.24$ m s^{-1} resulting in $z^+ = 3.6 \times 10^5$. The mean velocity was about 7.8 m s^{-1} and $\sigma_u/u_* = 3.1$.

C. Grass surface

The experiment was conducted from July 12 to 16 in 1995 at a grass site within the Blackwood division of the Duke Forest near Durham, North Carolina. The site is a 480-m by 305-m grass-covered forest clearing, and a mast, situated at 250 m and 160 m from the north-end and west-end portions of a 10-m Loblolly pine forest edge, respectively, was used to mount a triaxial ultrasonic anemometer (Gill Instruments/1012R2) at $z = 5.2$ m above the ground surface. The $h_c = 1.0$ m and LAI was around 1.5 m^2 m^{-2}. The sampling frequency and period per run were 56 Hz and 19.5 min, respectively. Further details can be found elsewhere [24]. The data reported here are for a 3.9-hour composite run made up of 12 consecutive runs with a $u_* = 0.45$ m s^{-1} resulting in $z^+ = 1.6 \times 10^5$. The mean velocity is about 4.1 m s^{-1} and $\sigma_u/u_* = 3.4$. The selected day here had the highest u_* values.

D. Pine forest

The experiment was conducted from October 6 to 10 in 1997 at the Blackwood Division of the Duke Forest near Durham, North Carolina, as part of a spatial variability in turbulent statistics campaign. The site is a uniformly aged managed loblolly pine plantation that extends at least 1 000 m in the north-south direction and 300 m to 600 m in the

east-west direction. The stand, originally grown from seedlings planted at 2.4-m by 2.4-m spacing in 1983 following clear cutting and burning, is approximately 14 m tall ($=h_c$). The measurements were performed at 5 Hz using a CSAT3 triaxial sonic anemometer (Campbell Scientific Inc., Logan, UT) positioned at $z = 15.5$ m above the forest floor. The LAI spatially varied from 2.65 to 4.56 $m^2\ m^{-2}$ across the stand [25]. The data reported here are for a 7-h composite run made up of 14 consecutive 30-min runs having a $u_* = 0.38$ m s^{-1} and resulting in $z^+ = 1.6 \times 10^5$. The mean velocity is about 1.1 m s^{-1} and $\sigma_u/u_* = 2.0$.

E. Hardwood forest

The hardwood (HW) experiment was conducted from June 16 to July 11 in 1996 at an 80- to 100-year-old second-growth Oak-Hickory forest situated at the Blackwood division of the Duke Forest, near Durham, North Carolina. The mean $h_c = 33$ m and the LAI is about 6 $m^2\ m^{-2}$. The velocity measurements were performed at 10 Hz using a symmetric three-axis ultrasonic anemometer (Gill Inst. Ltd.) positioned at the canopy top ($z = h_c$). Three days in which strong and steady winds occurred were used here, and are presented separately. Further details of the experiment can be found elsewhere [26]. The data reported here are for three separate days in which 5 consecutive hours were used per day resulting in a near-constant across days of $u_* = 0.63, 0.56, 0.57$ m s^{-1} and $z^+ = 7.4, 6.6, 6.7 \times 10^5$. The mean velocity for those runs were 1.9, 1.5, 2.0 m s^{-1} and $\sigma_u/u_* = 2.0$, 1.9, and 1.9, respectively.

Because of their differencing properties, OWTs are usually preferred for spectral analysis when some nonstationarity is expected (as is the case here). A drawback of OWT spectral analysis is their poor locality in the wavenumber domain due to dyadic scale arrangement. Hence, repeating the analysis in the Fourier domain allows some assessment of how robust the findings are to the analyzing basis functions. Figure 2 shows the Fourier spectra for E_u and E_w along with the -1 and $-5/3$ scaling exponents. The Fourier-based spectral density calculations are conducted using Welch's averaged modified periodogram method in which each time series is first divided into 10 sections with 50% overlap, then each section is processed using a Hamming-type window, and the resulting periodograms are computed and averaged with no prior detrending. Note that while the Fourier-based $E_u(k)$ exhibit an approximate -1 power-law scaling for all the sites, $E_w(k)$ does not. As earlier noted, $E_{\mathrm{TKE}}(k)$ is primarily driven by $E_u(k)$, not E_w. Hence, the -1 power law in $E_{\mathrm{TKE}}(k)$ is primarily due to the onset of a -1 power law in both E_u (shown here for reference) and E_v. Figure 3 also presents the Fourier-based E_{TKE} in premultiplied form to emphasize the range of scales exhibiting an approximate -1 power law. In this representation, a -1 power law appears as a constant. As with the orthonormal wavelet analysis, the inhomogeneous grass site does not exhibit a clear -1 power-law scaling in the expected range of normalized scales (shown as dashed vertical lines). The other experiments do exhibit an approximate -1

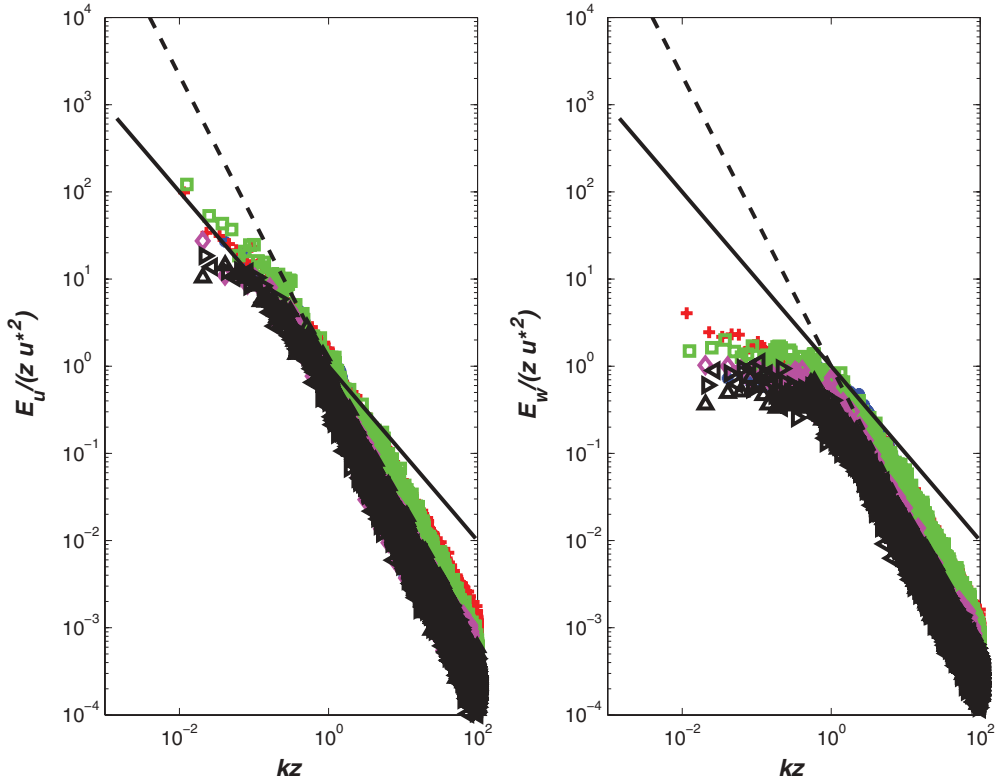

FIG. 2. (Color online) Measured normalized $E_u(k)$ and $E_w(k)$ using Fourier analysis. The normalizing velocity and length scales are measured u_* and z. The -1 (solid) and $-5/3$ (dashed) power laws are shown. The time domain is converted to wavenumbers using Taylor's frozen turbulence hypothesis and wavenumbers shown must be interpreted along the x direction, not three-dimensional.

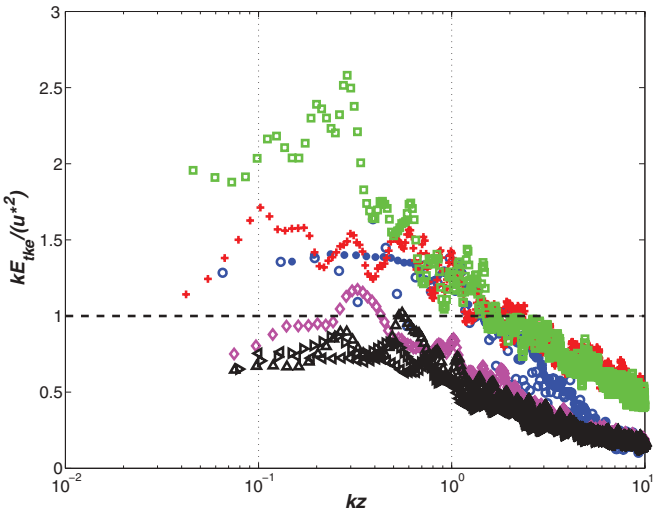

FIG. 3. (Color online) Measured normalized $E_{\mathrm{TKE}}(k)$ presented in premultiplied form.

power law, though variations around a constant C_{TKE} are not small across experiments (e.g., 0.6 to 1.5) for kz bounded between 0.1 and 1.0. Interestingly, the lower C_{TKE} values appear to be associated with rougher forested sites (pines and hardwoods) collected within the canopy sublayer while the higher C_{TKE} values are associated with the smooth-wall cases (open channel and ice sheet). Considering that (i) the atmosphere is nonuniformly heated during the day, (ii) the boundary layer dynamics cannot be ignored over several hours, (iii) Taylor's hypothesis is used in high-intensity flows and this usage is likely to distort the scale range upon which the -1 power law ought to be detected, and (iv) several data sets are collected just above tall forested sites and hence are within the canopy sublayer; some 20% variations in C_{TKE} within a given experiment or site is not surprising. Thus, the findings here do suggest that the results derived from the OWT analysis are robust to the analyzing basis function.

The geophysical flows here are characterized by an $H^+ > 100z^+$ or $z/H < 0.01$ resulting in at least one order of magnitude larger Reynolds number when compared to the super-pipe experiments in Ref. [16], while for the open channel flow, $z/H = 0.05 - 0.1$. The measurements in Fig. 1 suggest that E_{TKE} is roughly dominated by the exponents $-5/3$ (when $kz > 1$) and an approximate -1 (when $kz < 1$) with the k^{-1} scaling spanning just under one decade (except for the grass site). If the transition wavenumber from k^{-1} to $k^{-5/3}$ occurs sharply at $k_1 = 1/z$, as suggested by all the data here, then $C_{\mathrm{TKE}} = C_o k_v^{-2/3}$, which implies that $C_H = (4/3)C_o^{-3/2}$, a reasonable choice given that C_H should be of order unity and not dependent on k_v. For a $C_o = 1.55$, $C_H \approx 0.7$ and upon setting $k_v = 0.4$, $C_{\mathrm{TKE}} = 0.84$, consistent with a number of studies, including atmospheric surface layer flows [11]. The constant $C_{\mathrm{TKE}} = kE_{\mathrm{TKE}}/(u_*)^2$ of the -1 power-law range for the experiments in Fig. 1 deviates from 0.84 and varies from 0.5 to 1.4. The highest $C_{\mathrm{TKE}} = 1.4$ is for a highly inhomogeneous grass-covered forest clearing, where u_* may not be constant with z as assumed due to forest-edge disturbances. Moreover, E_v is mediated by nearby forest edges, while the lowest $C_{\mathrm{TKE}} = 0.5$ are for the tall hardwood forest canopy measurements ($z/h_c < 1.5$, where h_c is the mean canopy height). These measurements are impacted by momentum flux-transport terms [27] unbalancing the production and dissipation of TKE. Some laboratory measurements report $C_{\mathrm{TKE}} = 0.8$ for zero-pressure gradient [17], minor increases in $C_{\mathrm{TKE}} = 0.6$–0.8 with three orders of increase in Reynolds number [14], and lack of a k^{-1} scaling in adverse pressure-gradient flows but a presence of a k^{-1} scaling in the range of $0.06 < kz < 1$ for zero- and favorable-pressure gradients with $C_{\mathrm{TKE}} = 0.8$–1.0 [28]. In short, agreement between the phenomenological theory predictions for the -1 scaling and the plausible range of values of C_{TKE} appears consistent with a wide range of geophysical flows (at least, when the inhomogeneity is not too large as is the case with the grass site) and a large number of laboratory experiments.

IV. DISCUSSION

The present theory can also be linked to the framework of Townsend's attached eddies [29] in several ways. Both approaches assume an approximate balance between TKE production and dissipation rates. Moreover, the characteristic velocity of an eddy of size $kz = 1$ in this framework is given as $(kE_{\mathrm{TKE}})^{1/2} = \sqrt{C_{\mathrm{TKE}}}u_* \approx u_*$. Hence, analogous to the characteristic velocity of Townsend's attached eddies, eddies of size z here do have a representative velocity that is almost identical to u_*. The dissipation rate of e in Nikora [15] can also be reconciled with the spectral budget approach when assuming (i) infinite Reynolds number (needed when assuming the K41 spectrum represents all $k \in [k_1, \infty]$ with no intermittency or dissipation corrections for $kz \gg 1$), and (ii) very deep boundary layer allowing the extension of a single self-similar spectrum $E_{\mathrm{TKE}} = A\,k^{-a}$ to represent $k \in [0, k_1]$. Departures from these conditions can fingerprint absence of a k^{-1} in the E_{TKE}.

The proposed theoretical framework also allows us to analyze possible corrections to the k^{-1} scaling. One obvious departure is due to intermittency corrections to K41. Such corrections, either produced internally via heavy-tailed fluctuations from $\bar{\epsilon}$ [3,30] or externally via interactions between coherent structures and inertial scale eddies within the logarithmic region [31], can lead to a revised K41 spectrum whose simplest form is given as $C_i\overline{\varepsilon(k_1)}^{2/3}k'^{-5/3}(k'/k_1)^{-\mu}$, where C_i is a revised Kolmogorov constant. For this spectrum, and upon assuming an extensive $E_{\mathrm{TKE}} = Ak^{-a}$ range for $k \in [0, k_1]$, the spectral budget with intermittency corrections to K41 scaling at $kz > 1$ now requires that

$$2A\frac{k_1^{3-a}}{a-3} = \frac{(8+3\mu)}{6k_v^{2/3}C_H C_i^{1/2}}u_*^2 k_1^{2+\mu}. \tag{9}$$

It follows that $a = 1 - \mu$, resulting in a scaling not as steep as k^{-1}. For the internal intermittency corrections, a conventional $\mu \approx 0.06$ [4] results in $E_{\mathrm{TKE}} \sim k^{-0.94}$. If coherent structures or large-scale motion (including VLSM) interact with inertial size eddies (e.g., external intermittency) within the logarithmic region, then μ is expected to be larger than 0.06 and dependent on the Reynolds number, thereby weakening any evidence or universal signature of a k^{-1} scaling. Some studies reported

a $\mu \approx 0.15$ due to external intermittency effects [31,32], which would produce an $a \approx 0.85$ rather than near unity. As a result, the argument here suggests that modulations or even absence of a k^{-1} scaling may be partially attributed to "steepening" in the $k^{-5/3}$ for $kz > 1$ or even "censoring" its occurrence, as may occur when the viscous dissipation "cutoff" significantly intrudes into the inertial subrange. The converse is also true, if for $kz > 1$ the exponent describing the E_{TKE} is lower than $-5/3$ (i.e., $\mu < 0$), as may occur when the spectrum is gradually transitioning from production toward an inertial subrange regime, the spectral budget requires that $a > 1$. If a finite upper wavenumber bound is imposed on the K41 spectrum at the Kolmogorov dissipation wavenumber scale $k_d \sim \eta^{-1} = (\varepsilon/\nu^3)^{1/4}$ and ν_t is evaluated in the range $k \in [k_1, k_d]$ instead of $k \in [k_1, \infty]$, then ν_t/ν can be explicitly derived and is given as $\frac{\nu_t}{\nu} = \frac{3}{4}\sqrt{C_o}(\frac{u_* z}{\nu} - 1) \gg 1$, which results in $z^+ \gg 1 + 4/(3\sqrt{C_o}) \approx 2.78$. Assuming that this corresponds to $z^+ > 30$, a conventional value typically assumed to reach a fully turbulent boundary layer [33], any steepening of the spectrum due to viscous dissipation encroaching into the inertial subrange from higher wavenumbers would substantially increase this threshold by a factor of 2–4, based on numerical model calculations (not shown). These increases are consistent with the necessary conditions for the onset of a k^{-1} power law previously noted [17]. Finally, to naively include some effects originating from VLMS on $\bar{\varepsilon}$, it is useful to decompose the low k range on the left-hand side of Eq. (6) as

$$\int_0^{k_{\mathrm{low}}} 2E_{\mathrm{TKE}}(k')k'^2 dk' + \int_{k_{\mathrm{low}}}^{k_1} 2E_{\mathrm{TKE}}(k')k'^2 dk'. \qquad (10)$$

To further separate finite boundary depth from contributions originating from VLMS, it is initially assumed that the first term is small compared to the second and that $E_{\mathrm{TKE}} = A\,k^{-a}$ extends only from a finite $k_{\mathrm{low}} \sim (\alpha H)^{-1}$ to $k_1 \sim z^{-1}$, with $\alpha \leqslant 1$ being a fraction defining the size of the detached eddies in relation to H. This argument leads to

$$C_2 k_1^{3-a}[1 - (y)^{3-a}] = C_{\mathrm{TKE}} u_*^2 k_1^2, \qquad (11)$$

where $y = k_{\mathrm{low}}/k_1$ and $C_2 = 2A/(3-a)$. With $k_{\mathrm{low}} \sim (\alpha H)^{-1}$ necessitates a $z/H \ll \alpha$ at minimum to recover the k^{-1} scaling. This condition is similar to the condition that the overlap region between inner and outer layers be sufficiently wide to admit asymptotic matching arguments. If, on the other hand, the VLSM admit self-similar spectrum of the form $E_{\mathrm{TKE}} = B\,k^{-b}$ for $k \in [0, k_{\mathrm{low}}]$, then the revised Eq. (11) reads

$$C_2 k_1^{3-a}[1 - (y)^{3-a}] = C_3 k_1^2 \left[1 - C_4\,(y)^2\, k_{\mathrm{low}}^{1-b}\right], \qquad (12)$$

where $C_3 = C_{\mathrm{TKE}} u_*^2$ and $C_4 = 2B/[(3-b)C_3]$. Again, if $k_{\mathrm{low}} \ll k_1$, then the onset of k^{-1} requires that $3 - a = 2$ (or $a = 1$) provided $b < a$. However, for VLSM, the $B \sim u_*^2\,(H_{\mathrm{VLSM}})^{1-b}$ and noting that $C_3 \sim u_*^2$ results in a new and far more stringent condition for the onset of the k^{-1}, given as

$$\left(\frac{z}{H}\right)^2 \left(\frac{H_{\mathrm{VLSM}}}{H}\right)^{1-b} \ll \alpha^{3-b}. \qquad (13)$$

A number of studies already reported $H_{\mathrm{VLSM}}/H \sim 10$ [19,34]. For an $\alpha = 0.8$, $b = 0$, and $H_{\mathrm{VLSM}}/H \sim 10$ results in $z/H \ll 0.23$. Hence, the small range of z/H needed is not only to ensure an adequate overlap region between inner and outer layers as earlier noted, but also to minimize modulations originating from VLSM. In fact, these modulations require an even more stringent z/H range. It should be noted that detecting the spectral contributions of VLMS in Fig. 1 for the geophysical flows may be complicated by the fact that the spectra are composites of several hours during the day where H may be evolving in time. It is difficult to separate VLSM from nonstationarity in H within such setup.

V. CONCLUSION

The multiple mechanisms explaining a "-1" power-law scaling at low wavenumbers in E_{TKE} (and in E_u) of wall-bounded turbulence can be unified via a phenomenological theory rooted in Heisenberg's eddy viscosity approach. The theoretical framework accounts for intermittency corrections within the inertial subrange and the presence of very-large scale motion, resulting in exponents not as steep as k^{-1}, at least for eddy sizes larger than z but much smaller than H.

ACKNOWLEDGMENTS

Support from the US Department of Energy through the office of Biological and Environmental Research (BER) Terrestrial Ecosystem Science (TES) program (Grant No. DE-SC0006967), the US National Science Foundation (Grants No. NSF-CBET 103347, No. NSF-EAR-10-13339, and No. NSF-AGS-1102227), the US Department of Agriculture (Grant No. 2011-67003-30222), and EPSRC UK (Grant No. EP/G056404/1) supported project "High-resolution numerical and experimental studies of turbulence-induced sediment erosion and near-bed transport" are acknowledged.

APPENDIX: A SIMPLIFIED SPECTRAL BUDGET

Consider the Reynolds-averaged TKE budget in a stationary and planar-homogeneous flow with no mean vertical velocity (i.e., $\bar{W} = 0$) given by Ref. [35]

$$\frac{\partial e}{\partial t} = 0 = -\overline{u'w'}\frac{d\bar{U}}{dz} - \frac{\partial}{\partial z}(\overline{w'e} + \overline{w'p'}) - \bar{\varepsilon}, \qquad (A1)$$

where e is, as before, the turbulent kinetic energy $= \frac{1}{2}(\sigma_u^2 + \sigma_v^2 + \sigma_w^2)$, $\bar{U}$ is the mean velocity at z, $\overline{u'w'}$ is the momentum flux, and the first, second, and third terms are the mechanical production, the TKE transport by turbulence and pressure-velocity interactions, and viscous dissipation, respectively. In the equilibrium or logarithmic region of a boundary-layer, the transport terms are usually small resulting in a near-balance between production and dissipation of TKE as was assumed by Townsend and many others [35].

If the mean TKE dissipation rate ($=\bar{\varepsilon}$) is a conservative quantity in the energy cascade, then a spectral budget can be

derived as [36]:

$$\bar{\varepsilon} = -\frac{d\bar{U}}{dz}\int_k^\infty \tau(p)dp + F(k) + 2\nu\int_0^k p^2 E_{\mathrm{TKE}}(p)dp, \tag{A2}$$

where the first, second, and third terms represent the production of turbulence in the range of $[k,\infty]$, the transfer of turbulence energy in the range $[k,\infty]$, and the viscous dissipation in the range of $[0,k]$. Here, the functions $F(k)$, $\tau(k)$, and $E_{\mathrm{TKE}}(k)$ are averaged over all directions in the wavevector space as the turbulence is nonisotropic, and $k=\sqrt{k_x^2+k_y^2+k_z^2}$, where x, y, and z are the longitudinal, lateral, and vertical directions, respectively. The treatment of $d\bar{U}/dz$ as a constant external to the spectral budget is a major simplification permitting analytical tractability. Two asymptotic conditions must now be satisfied so that this spectral budget recovers the classical results of turbulent boundary layers in the equilibrium or logarithmic regions. The first is that at $k=0$, $F(0)=0$, and

$$\bar{\varepsilon} = -\frac{dU}{dz}\int_0^\infty \tau(p)dp = -\frac{d\bar{U}}{dz}\overline{(u'w')}, \tag{A3}$$

so that $\int_0^\infty \tau(p)dp = \overline{u'w'}$. This is the main result for the equilibrium region as earlier noted, necessitating a balance between mechanical production and $\bar{\varepsilon}$. The second is that as $k\to\infty$, $F(\infty)\to 0$, and

$$\bar{\varepsilon} \approx 2\nu\int_0^\infty p^2 E_{\mathrm{TKE}}(p)dp, \tag{A4}$$

or the mean TKE dissipation rate is primarily occurring via the viscous term at very large k.

As noted in the main text, the Heisenberg model for $F(k)$ is given as

$$F(k) = \nu_t(k)\overline{|\mathrm{curl}\,\tilde{u}|^2} \approx 2\nu_t(k)\int_0^k p^2 E_{\mathrm{TKE}}(p)dp, \tag{A5}$$

where the eddy viscosity coefficient $\nu_t(k)$ is produced by the motion of eddies with wavenumbers greater than k, and $\tilde{u}$ is the "macro-scale" component of the velocity. With these approximations, the spectral budget can be expressed as

$$\varepsilon(k) = \bar{\varepsilon} + \frac{d\bar{U}}{dz}\int_k^\infty \tau(p)dp = 2[\nu_T(k)+\nu]\int_0^k p^2 E_{\mathrm{TKE}}(p)dp. \tag{A6}$$

Noting that

$$\int_0^\infty \tau(p)dp = \overline{u'w'} = -\bar{\nu}_t\frac{d\bar{U}}{dz}, \tag{A7}$$

and assuming an analogous gradient-diffusion closure in the spectral domain yields,

$$\frac{d\bar{U}}{dz}\int_k^\infty \tau(p)dp \approx A_t\nu_t(k)\left(\frac{d\bar{U}}{dz}\right)^2, \tag{A8}$$

where A_t is a normalizing constant needed to ensure that Eq. (A3) is satisfied for a given $E_{\mathrm{TKE}}(p)$ shape, and as before,

$$\nu_t(k) = C_H\int_k^\infty \sqrt{\frac{E_{\mathrm{TKE}}(p)}{p^3}}dp, \tag{A9}$$

is the Heisenberg eddy viscosity. If $E_{\mathrm{TKE}}(p) = C_o\bar{\varepsilon}^{2/3}p^{-5/3}$ is also assumed for $p\in[1/z,\infty]$, then

$$\nu_t(k) = \frac{3}{4}C_H\sqrt{C_o}\bar{\varepsilon}^{1/3}k^{-4/3}. \tag{A10}$$

Noting that in the equilibrium layer, $d\bar{U}/dz = u_*/(k_v z)$, the production term associated with the spatial gradients can now be estimated and is given as

$$\frac{d\bar{U}}{dz}\int_{1/z}^\infty \tau(p)dp \approx -A_t C_H\frac{3\sqrt{C_o}}{4k_v^{4/3}}\frac{u_*^3}{k_v z}. \tag{A11}$$

Hence, the spectral budget equation in the vicinity of $kz\approx 1$ is

$$\bar{\varepsilon} + \frac{d\bar{U}}{dz}\int_k^\infty \tau(p)dp \approx \left(\frac{1}{k_v}u_*^3 k\right)[A'], \tag{A12}$$

where

$$A' = \left[1 - A_t C_H\frac{3\sqrt{C_o}}{4k_v^{3/4}}\right]. \tag{A13}$$

The original spectral budget equation is now given as

$$A'\frac{1}{k_v}u_*^3 k \approx 2(\nu_t(k)+\nu)\int_0^k p^2 E_{\mathrm{TKE}}(p)dp. \tag{A14}$$

Depending on the value of A_t, the spatial gradient term remains significant at $kz\approx 1$ and may not be neglected, but the fact that it scales with $u_*^3/(k_v z)$, as shown here, allows us to recover the original argument leading to the -1 power law to within a constant A'. To further illustrate, note that upon adopting the Heisenberg representation of the eddy-viscosity results in

$$A'\frac{1}{k_v}u_*^3 k \approx \left[2C_H\int_k^\infty \sqrt{\frac{E_{\mathrm{TKE}}(p)}{p^3}}dp\right]\int_0^k p^2 E_{\mathrm{TKE}}(p)dp, \tag{A15}$$

where $E_{\mathrm{TKE}}(p) = C_o\bar{\varepsilon}^{2/3}p^{-5/3}$ is again assumed for $p\in[1/z,\infty]$, but a general power-law spectrum of the form $E_{\mathrm{TKE}}(p) = Ap^\alpha$ is assumed for $p\in[0,\ 1/z]$. This result differs from the original version of the manuscript only by a constant A'.

[1] A. N. Kolmogorov, Proc. R. Soc. London A **434**, 15 (1991).

[2] A. N. Kolmogorov, Proc. R. Soc. London A **434**, 9 (1991).

[3] A. N. Kolmogorov, J. Fluid Mech. **13**, 82 (1962).

[4] U. Frisch, in *Turbulence: The Legacy of A.N. Kolmogorov* (Cambridge University Press, New York, 1995), p. 296.

[5] G. Katul and C. R. Chu, Boundary-Layer Meteorology **86**, 279 (1998).

[6] H. Lu and F. Porté-Agel, Phys. Fluids **22**, 015109 (2010).
[7] R. Stoll and F. Porte-Agel, Boundary-Layer Meteorology **118**, 169 (2006).
[8] P. Drobinski, P. Carlotti, J. L. Redelsperger, R. M. Banta, V. Masson, and R. K. Newsom, J. Atmos. Sci. **64**, 137 (2007).
[9] C. M. Tchen, J. Res. Natl. Bureau Stand. **50**, 51 (1953).
[10] C. M. Tchen, Phys. Rev. **93**, 4 (1954).
[11] B. A. Kader and A. M. Yaglom, in *Turbulence and Coherent Structures*, edited by O. Metais and M. Lesieur (Kluwer Academic Press, New York, 1991), pp. 388–412.
[12] A. E. Perry, S. Henbest, and M. S. Chong, J. Fluid Mech. **165**, 163 (1986).
[13] J. C. R. Hunt and J. F. Morrison, Eur. J. Mech. B Fluids **19**, 673 (2000).
[14] I. Marusic, B. J. McKeon, P. A. Monkewitz, H. M. Nagib, A. J. Smits, and K. R. Sreenivasan, Phys. Fluids **22**, 065103 (2010).
[15] V. Nikora, Phys. Rev. Lett. **83**, 734 (1999).
[16] J. F. Morrison, W. Jiang, B. J. McKeon, and A. J. Smits, Phys. Rev. Lett. **88**, 214501 (2002).
[17] T. B. Nickels, I. Marusic, S. Hafez, and M. S. Chong, Phys. Rev. Lett. **95**, 074501 (2005).
[18] G. J. Kunkel and I. Marusic, J. Fluid Mech. **548**, 375 (2006).
[19] A. J. Smits, B. J. McKeon, and I. Marusic, Annu. Rev. Fluid Mech. **43**, 353 (2011).
[20] W. Heisenberg, Proc. R. Soc. London A **195**, 402 (1948).
[21] J. Jimenez, Physica A **263**, 252 (1999).
[22] N. Marati, C. Casciola, and R. Piva, J. Fluid Mech. **521**, 191 (2004).
[23] D. Cava, U. Giostra, and M. Tagliazucca, Boundary-Layer Meteorol. **100**, 421 (2001).
[24] G. Katul, C. Hsieh, and J. Sigmon, Boundary-Layer Meteorol. **82**, 49 (1997).
[25] G. Katul, C. Hsieh, D. Bowling, K. Clark, N. Shurpali, A. Turnipseed, J. Albertson, K. Tu, D. Hollinger, B. Evans, B. Offerle, D. Anderson, D. Ellsworth, C. Vogel, and R. Oren, Boundary Layer Meteorol. **93**, 1 (1999).
[26] G. Katul, C. Hsieh, G. Kuhn, D. Ellsworth, and D. Nie, J. Geophys. Res. **102**, 13409 (1997).
[27] D. Poggi, G. Katul, and J. Albertson, Boundary-Layer Meteorol. **111**, 589 (2004).
[28] O. Turan, R. Azad, and S. Z. Kassab, Phys. Fluids **30**, 3463 (1987).
[29] A. Townsend, *The Structure of Turbulent Shear Flow* (Cambridge University Press, Cambridge, 1976).
[30] U. Frisch, P. L. Sulem, and M. Nelkin, J. Fluid Mech. **87**, 719 (1978).
[31] V. R. Kuznetsov, A. A. Praskovsky, and V. A. Sabelnikov, J. Fluid Mech. **243**, 595 (1992).
[32] G. Katul, A. Porporato, D. Cava, and M. Siqueira, Physica D **215**, 117 (2006).
[33] D. Poggi, A. Porporato, and L. Ridolfi, Phys. Fluids **15**, 35 (2003).
[34] I. Marusic, R. Mathis, and N. Hutchins, Science **329**, 193 (2010).
[35] S. Pope, in *Turbulence Flows* (Cambridge University Press, Cambridge, UK, 2000) p. 779.
[36] J. Hinze, in *Turbulence: An Introduction to Its Mechanism and Theory* (McGraw Hill, New York, 1959) p. 586.